PHYSICAL REVIEW A **72**, 013801 (2005)

Production of superpositions of coherent states in traveling optical fields with inefficient photon detection

H. Jeong, A. P. Lund, and T. C. Ralph
Center for Quantum Computer Technology, Department of Physics, University of Queensland, St Lucia, Qld 4072, Australia
(Received 21 September 2004; revised manuscript received 24 November 2004; published 1 July 2005)

We develop an all-optical scheme to generate superpositions of macroscopically distinguishable coherent states in traveling optical fields. It nondeterministically distills coherent-state superpositions (CSS's) with large amplitudes out of CSS's with small amplitudes using inefficient photon detection. The small CSS's required to produce CSS's with larger amplitudes are extremely well approximated by squeezed single photons. We discuss some remarkable features of this scheme: it effectively purifies mixed initial states emitted from inefficient single-photon sources and boosts negativity of Wigner functions of quantum states.

DOI: 10.1103/PhysRevA.72.013801 PACS number(s): 42.50.Dv, 03.65.Ta, 03.67.Mn

I. INTRODUCTION

The Schrödinger's cat paradox is a famous illustration of the principle of superposition in quantum theory [1]. It poses the question of whether a classical object on the macroscopic level can be in a state of quantum superposition. The component states composing such a superposition should give macroscopically distinct measurement outcomes [2,3]. A superposition of two optical coherent states with sufficiently large amplitudes of a π-phase difference is considered a realization of such a macroscopic superposition and often called a "Schrödinger cat state."

Recently, such coherent-state superpositions (CSS's) in free propagating optical fields have been found to be useful for various applications to quantum information processing [4–13]. Quantum teleportation [4–8], quantum computation [9–11], entanglement purification [12] and concentration [5], error correction [13], and remote entangling [8] have been extensively studied with CSS's. In particular, it was shown that quantum computation can be realized using only linear optics and photon counting, given prearranged CSS's as resources [10,11]. In this approach, a qubit is defined to be a superposition of two coherent states, and all four Bell states can be perfectly well discriminated by photon counting measurements and a beam splitter [5,12]. This enables one to construct quantum gates in a relatively simple way based on the teleportation protocol [11]. The amplitudes of coherent states for qubits and resource CSS's should be carefully chosen for efficiency of quantum information processing. The CSS's of amplitude $\alpha > 2$ are required as resources for efficient quantum computation with simple optical networks [11].

It is known to be extremely hard to generate a free propagating CSS using current technology. It is well known that the CSS can be generated from a coherent state by a nonlinear interaction in a Kerr medium [14]. However, Kerr nonlinearity of currently available nonlinear media is extremely small compared with the level required to generate a CSS and attenuation in the media is not negligible [15].

Some alternative methods have been studied to generate a superposition of macroscopically distinguishable states based upon conditional measurements [16,17]. A crucial drawback of these schemes is that highly efficient photon detection is necessary. The schemes of both Song *et al.* [16] and Dakna *et al.* [17] require photon number resolving measurements, which is extremely demanding using current technology. Some other schemes [18] require many single-photon detectors instead of one n-photon counting detector. Even though it is known that many perfect single-photon detectors enable one to perform nearly perfect n-photon counting, such a scheme would suffer a similar difficulty due to detection inefficiency of many single-photon detectors. Many perfect detectors used to produce macroscopic superpositions can be replaced with two n-photon Fock states and two perfect detectors [19]. This employs another unavailable factor (two n-photon Fock states) by current technology. A modified scheme [20] of Ref. [16] suggested by Montina can be robust to detection inefficiency under certain conditions where success probability is extremely low and amplitudes of the generated CSS's are small such as $\alpha < 1$. None of the above schemes based on conditional measurements are currently feasible to generate CSS's with high fidelity, the main difficulty being the unavoidable inefficiency of photon detection.

Cavity quantum electrodynamics has been studied to enhance nonlinear effects to generate macroscopic superpositions [21]. Some success has been reported in creating such superposition states within high-Q cavities in the microwave [22] and optical [23] domains. However, most of the schemes suggested for quantum information processing with coherent states [4–13] require *free propagating* CSS's.

Recently, it was shown that free propagating optical CSS's with amplitude up to $\alpha = 2.5$ and fidelity $F > 0.99$ can be generated with squeezed single photons and simple all-optical operations [24], where neither efficient photon detection nor $\chi^{(3)}$ nonlinear interactions are required. It was also found to be resilient to photon production inefficiency to some extent as its first step effectively purifies initial mixed states emitted from an inefficient single photon source [24]. In a more general sense, these examples reveal that the first excited energy eigenstates can be converted to a superposition of macroscopically distinguishable states by linear operations and projections.

In this paper, we extensively analyze the scheme in Ref. [24] and find that its purification effects can last for further

steps. The nondeterministic CSS amplification scheme is found to boost the nonclassicality of quantum states: even very small amount of negativity can be drastically increased by this process. It is also pointed out that the single-photon source is not necessary to obtain squeezed single photons if another nondeterministic technique, photon subtraction [25] as demonstrated in a recent experiment [26], is employed.

This paper is organized as follows. In Sec. II, We briefly define and discuss the CSS as a macroscopic superposition state with Schrödinger's cat paradox. In Sec. III, it is shown that a CSS with a small coherent amplitude ($\alpha \leqslant 1.2$) and high fidelity ($F > 0.99$) can be deterministically generated by squeezing a single photon. The discussion is motivated by the approach of Ref. [16]. The Wigner functions of squeezed single photons and CSS's are analytically obtained, and they are compared to visualize the effects of squeezing on single photons. In Sec. IV, we fully analyze and discuss the CSS amplification scheme with beam splitters, auxiliary coherent fields, and inefficient detectors. Section V combines the two ideas from Secs. III and IV to produce CSS's with amplitude $\alpha > 2$. Weak squeezing, beam mixing with an auxiliary coherent field, and photon detecting with threshold detectors are enough to generate a CSS with amplitude up to $\alpha = 2.5$ and high fidelity ($F > 0.99$) given a single-photon source. Pufication effects for an inefficient single-photon source are another remarkable aspect of our scheme, which will be discussed in Sec. VI particularly for multiple iterations of the process. We conclude with some final remarks in Sec. VII. A recent experiment by Wenger *et al.* [26] is briefly addressed from the viewpoint of CSS generation. We emphasize that single-photon sources are not necessary to generate CSS's of $\alpha > 2$ employing the photon subtraction technique with our amplification scheme.

II. SUPERPOSITIONS OF COHERENT STATES AS MACROSCOPIC SUPERPOSITIONS—CAN THEY BE CALLED "SCHRÖDINGER CATS"?

A CSS can be defined as

$$|\mathrm{CSS}_{\varphi}(\alpha)\rangle = N_{\varphi}(\alpha)(|\alpha\rangle + e^{i\varphi}|-\alpha\rangle), \tag{1}$$

where $N_{\varphi}(\alpha)$ is a normalization factor, $|\pm\alpha\rangle$ is a coherent state of amplitude $\pm\alpha$, and φ is a real local phase factor. The amplitude α is assumed to be real for simplicity without loss of generality. In this paper we refer to the magnitude of α as the size of the CSS. Note that CSS's such as $|\mathrm{CSS}_{\pm}(\alpha)\rangle = N_{\pm}(\alpha)(|\alpha\rangle \pm |-\alpha\rangle)$ are called even and odd CSS's respectively, because the even (odd) CSS always contains an even (odd) number of photons.

In Schrödinger's paradox, a classical object (cat) is in a superposition of two macroscopically distinguishable states (alive and dead). Leggett and Garg have shown the incompatibility between quantum-mechanical prediction and macroscopic realism for a macroscopic superposition state [2]. The same kind of discussions have been made by Reid to show violation of Bell's inequality when local realism is macroscopically defined [3]. A CSS is in a macroscopic superposition state when its amplitude is appropriately large. It is often referred to as a "Schrödinger cat state" or simply "cat state" albeit there exists some dispute over the term.

There are probably two conspicuous characteristics of CSS's which may justify the title Schrödinger cat states. First, coherent states are known as the most classical states among pure states. The coherent states were originally suggested by Schrödinger as a quantum analogy of classical particles [27]. A classical particle can be represented as a point in the phase space while it is prohibited by the uncertainty principle for a quantum state. A coherent state provides the most pointlike description of a quantum particle in the phase space among all quantum states. Furthermore, the coherent states do not change their localized shapes as they move in a harmonic oscillator potential. Their Wigner functions are positive definite and their P function exists even though they are δ functions [28].

Second, two coherent states are macroscopically distinguishable when they are well separated in the phase space. Homodyne detection can be considered a macroscopic measurement as it does not resolve individual quanta (photon). The error probability P_e of discriminating two coherent states $|\alpha\rangle$ and $|-\alpha\rangle$ by a homodyne detection is [29]

$$P_e = \mathrm{Erf}(\sqrt{2}\alpha) - \frac{1}{2}, \tag{2}$$

where $\mathrm{Erf}(x)$ is the error function. The error probability P_e corresponds to the probability of a wrong discernment by the homodyne detection due to the overlap between the two coherent states. The probability P_e is extremely small as $P_e < 3.2 \times 10^{-5}$ for $\alpha > 2$. In such a case, a CSS in Eq. (1) can be considered a superposition between two macroscopically distinguishable states of a classical system.

The first characteristic explained above could be more or less weaker than the second one as a justification for Schrödinger cat states being an alternative title of CSS's. The coherent states are, of course, still far from typical classical objects. It was shown that quantum key distribution using coherent states and homodyne measurements is secure against any individual eavesdropping attack [30]. It has also been argued that a weak measurement of the squared quadrature observable may yield negative values for coherent states [31].

The virtual cat in Schrödinger's paradox is, to be more precise, entangled with a microscopic quantum object while a CSS in Eq. (1) is in a single mode superposition. However, an entangled coherent state

$$|\mathrm{ECS}\rangle \propto |\alpha\rangle|\beta\rangle + e^{i\varphi}|-\alpha\rangle|-\beta\rangle \tag{3}$$

can be simply generated by dividing a CSS using a beam splitter. Such an entanglement in Eq. (3) of macroscopically distinguishable states is perhaps more closely aligned with Schrödinger's original concept [1].

We have shown that the error probability of discriminating between two coherent states, $|\alpha\rangle$ and $|-\alpha\rangle$, is extremely small for $\alpha > 2$, which justifies the CSS as, at least, a macroscopic superposition state. This value ($\alpha > 2$) is also appro-

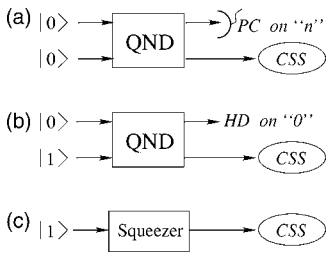

FIG. 1. A schematic of the simplification of the CSS generation. PC represents photon counting and HD represents homodyne detection. (a) Conditional production using QND with photon counting, (b) conditional production using QND with homodyne detection, and (C) deterministic production only by squeezing a single photon.

priate for quantum computation using optical coherent states [10]. Therefore, we are particularly interested in generating CSS's of $\alpha > 2$ in this paper.

III. GENERATION OF SMALL COHERENT-STATE SUPERPOSITIONS

There have been some trials to generate macroscopic superpositions using the optical parametric amplifier and a single-photon source [16,32]. In this section, we show how a previous scheme [16] to generate macroscopic superpositions can be significantly simplified so that small CSS's with high fidelity can be deterministically generated simply by squeezing single photons (see Fig. 1).

A. Simplified generation of small coherent-state superpositions

The key idea presented in this section is motivated by the scheme described in [16]. This scheme uses a nonlinear coupling between two optical modes which realizes a quantum nondemolition (QND) measurement on the $\hat{Y}$ quadrature of one mode. This is done by coupling the mode containing the signal to another ancillary mode as described in [33]. We define the quadrature operators of a single mode in terms of the usual creation and annihilation operators as $\hat{X}=\hat{a}+\hat{a}^{\dagger}$ and $\hat{Y}=-i(\hat{a}-\hat{a}^{\dagger})$ so that $[\hat{X},\hat{Y}]=2i$ and hence

$$\sqrt{\langle \Delta \hat{X}^2 \rangle \langle \Delta \hat{Y}^2 \rangle} = 1. \tag{4}$$

So as to avoid confusion between the two quantized modes of the EM field in the QND appratus, the mode which the QND measurement is performed is called the signal mode and the mode it interacts with to assist with the measurement is called the meter mode. Also the operators associated with the observables of these modes are labeled with subscript s for signal and m for meter. The device described in [33] uses the two polarization modes of a single spatial mode as the signal and meter modes. For example, the horizontal polarization might contain the signal and vertical polarization the meter. The meter mode is usually assumed to be prepared in the vacuum state. The two polarization modes are mixed by a waveplate by an angle θ. Then two-mode squeezing is performed between the two polarization modes by a $\chi^{(2)}$ nonlinear crystal. The squeezing parameter r is determined by the power applied to a pump beam which creates a squeezed vacuum in the absence of any input signal. Finally the polarizations are mixed by a waveplate by the same angle θ. The evolution through this device is unitary and can be represented by a unitary operator $\hat{U}$. When the squeezing parameter and waveplate mixing angle are related by $\tanh r = \sin 2\theta$ (called the QND condition) then the quadrature operators transform as [16]

$$\begin{pmatrix} \hat{X}_s \\ \hat{X}_m \end{pmatrix}_o = \hat{U}^{\dagger} \begin{pmatrix} \hat{X}_s \\ \hat{X}_m \end{pmatrix}_i \hat{U} \begin{pmatrix} 1 & -2\sinh r \\ 0 & 1 \end{pmatrix} \begin{pmatrix} \hat{X}_s \\ \hat{X}_m \end{pmatrix}_i, \tag{5}$$

$$\begin{pmatrix} \hat{Y}_s \\ \hat{Y}_m \end{pmatrix}_o = \hat{U}^{\dagger} \begin{pmatrix} \hat{Y}_s \\ \hat{Y}_m \end{pmatrix}_i \hat{U} \begin{pmatrix} 1 & 0 \\ 2\sinh r & 1 \end{pmatrix} \begin{pmatrix} \hat{Y}_s \\ \hat{Y}_m \end{pmatrix}_i. \tag{6}$$

From these relations it is possible to see that the $\hat{Y}_s$ operator is left unchanged through the apparatus but the $\hat{Y}_m$ operator is mixed with the $\hat{Y}_s$ operator. This allows information about the $\hat{Y}$ quadrature of the signal to be gathered from the meter mode while leaving the signal itself undisturbed. Note that to satisfy the uncertainty relation from Eq. (4) the $\hat{X}$ quadrature of the signal output is not identical to its input.

In attempting to generate CSS's, the scheme in [16] suggests preparing the signal (and meter) in the vacuum state. Then apply the QND apparatus just described and perform a photon number measurement on the meter. The signal output is only accepted when a predefined number of photons is registered in the measurement. It is shown heuristically in [16] that one would expect a CSS to be generated when $r \gg 1$. When an odd number of photons is counted in the meter mode the output is close to an odd CSS and when an even number of photons is counted the output is close to an even CSS.

The scheme described in [16] relies on photon counting measurements to post-select the desired output state. This ability to conditionally select the output induces the required nonlinearity. However, this requires efficient detection and photon number measurements which are difficult to implement. One possible resolution to this would be to use detection schemes which can be made to perform efficiently when post-selecting the output state. We suggest here to use homodyne detection which might be performed with much higher efficiency than photon counting measurements.

Homodyne measurements are effectively a measurement of the $\hat{X}$ or $\hat{Y}$ quadratures depending on the phase of a reference signal. The eigenvalue spectrum of these operators is continuous which makes post-selection on a particular value have little meaning as that one value is infinitesimally small in the set of all possible values. For example, one could measure $\hat{X}$ and select the result for eigenvalue zero but one could never be sure that the result was precisely zero. To circumvent this problem one can use the technique shown in [35] which accepts events within a given window of possible values and rejects all others.

In order to produce states similar to those in [16] by homodyne post-selection we suggest preparing the signal mode in a Fock state, then post-select by performing a homodyne measurement on the meter mode after the QND apparatus. The condition to accept the output of the signal is if the measurement was in the range $(-\delta, \delta)$ where δ is some small constant. We provide a heuristic description in a similar fashion to that in [16] but perform a more complete analysis on a simplification that naturally arises when trying to write down the output state.

The heuristic description proceeds by expanding the signal-mode photon number operator in terms of the quadrature operators—i.e.,

$$\hat{n}_{si} = \frac{\hat{X}_{si}^2}{4} + \frac{\hat{Y}_{si}^2}{4} - \frac{\hat{I}_{si}}{2}, \tag{7}$$

where the subscript s represents the fact that the operator represents the signal mode and the subscript i for input. The QND apparatus leaves the $\hat{Y}$ quadrature of the signal unchanged by Eq. (6), so

$$\hat{n}_{si} = \frac{\hat{X}_{si}^2}{4} + \frac{\hat{Y}_{so}^2}{4} - \frac{\hat{I}_{si}}{2}. \tag{8}$$

Here the subscript o represents the operator for the output mode. Now the $\hat{X}$ quadrature of the signal transforms as

$$\hat{X}_{so} = \hat{X}_{si} - 2 \sinh r \hat{X}_{mi} \tag{9}$$

and the $\hat{Y}$ quadrature of the meter transforms as

$$\hat{Y}_{mo} = \hat{Y}_{mi} + 2 \sinh r \hat{Y}_{si}, \tag{10}$$

where the subscript m represents the meter mode. We now require a post-selective measurement on $\hat{Y}_{mo}$. We use a semiclassical approach to complete this heuristic description by converting operators back into classical variables. In terms of the semiclassical quadrature variables, the effect of the post-selective measurement can be included by setting $Y_{mo}=0$. So we can write the signal output as

$$Y_{so} = Y_{si} = -\frac{1}{2 \sinh r} Y_{mi}. \tag{11}$$

From this equation we can see that after post-selection the Y quadrature of the signal output is a scaled form of the Y quadrature to the meter input. Substituting this expression into Eq. (7) and rearranging for the signal output X quadrature one obtains

$$X_{so} = \pm \sqrt{4n_{si} + 2 - \left(\frac{Y_{mi}}{2 \sinh r}\right)^2} - 2 \sinh r X_{mi}. \tag{12}$$

Here we consider n_{si} the semiclassical form of the signal input photon number operator which will only take on integer values. The meter input is a vacuum state and hence the X and Y quadratures contain Gaussian noise. The signal input contains a definite photon number. So the first term under the square root will act like a constant. The second term will have some scaled Gaussian random noise and so will the term outside the square root. However, the multivalued nature of the square root gives the two-peaked behavior required. This completes our heuristic description.

In this paper we will not perform an in-depth analysis of this device in full to rigorously confirm the results of the heuristic argument just given. However, a complete analysis has been performed which confirms this description [34]. Here we will analyze a simplification of this device which has similar functionality and will prove fruitful towards achieving our goal of a simplified experiment.

One can show that the unitary operator which generates the operator transformation equations (5) and (6) of the QND apparatus is

$$\hat{U} = e^{i2 \sinh(r) \hat{X}_m \hat{Y}_s}. \tag{13}$$

Now consider this operator acting on the initial state where the signal is in a Fock state and the meter is in the vacuum state—i.e.,

$$\hat{U} |n\rangle_s |0\rangle_m. \tag{14}$$

Inserting two instances of the identity, one expanded over the eigenstates of $\hat{X}_m$ and the other eigenstates of $\hat{Y}_s$, we have

$$\int_{-\infty}^{\infty} \mathrm{d}x_m \int_{-\infty}^{\infty} \mathrm{d}y_s e^{i2 \sinh(r) \hat{X}_m \hat{Y}_s} |y_s\rangle |x_m\rangle \langle y_s| n\rangle \langle x_m|0\rangle. \tag{15}$$

When expressions for the inner products are substituted, this equation becomes

$$\mathcal{N}_n N_\sigma \int_{-\infty}^{\infty} \mathrm{d}x_m \int_{-\infty}^{\infty} \mathrm{d}y_s e^{i2 \sinh(r) x_m y_s} e^{-y_s^2/2} H_n(y_s) e^{-x_m^2/2\sigma} |y_s\rangle |x_m\rangle, \tag{16}$$

where $\mathcal{N}_n$ and N_σ are normalization factors for the nth photon term and a Gaussian with standard deviation σ, respectively, and $H_n(y_s)$ is the nth Hermite polynomial. The process of projecting onto the $\hat{Y}_m=0$ state can be included by taking the inner product of this state with the state on the meter mode alone $\mathrm{d}Y \langle y_m=0|$. This leaves us with a $\langle y_m=0|x_m\rangle$ inside the integral. This term is $e^{i0 \cdot x_m}=1$. Hence the post-selected output state is

$$\mathrm{d}Y \mathcal{N}_n N_\sigma \int_{-\infty}^{\infty} \mathrm{d}x_m \int_{-\infty}^{\infty} \mathrm{d}y_s e^{i2 \sinh(r) x_m y_s} e^{-y_s^2/2} H_n(y_s) e^{-x_m^2/2\sigma} |y_s\rangle. \tag{17}$$

When the terms involving x_m are grouped together and factored by completing the square and the integration over x_m is performed one is left with

$$\mathrm{d}Y \mathcal{N}_n \int_{-\infty}^{\infty} \mathrm{d}y_s e^{-[1+4\sigma \sinh^2(r)] y_s^2/2} H_n(y_s) |y_s\rangle. \tag{18}$$

This can be a written a little clearer if we set $\kappa = \sqrt{1+4\sigma \sinh^2(r)}$. Hence the signal output is

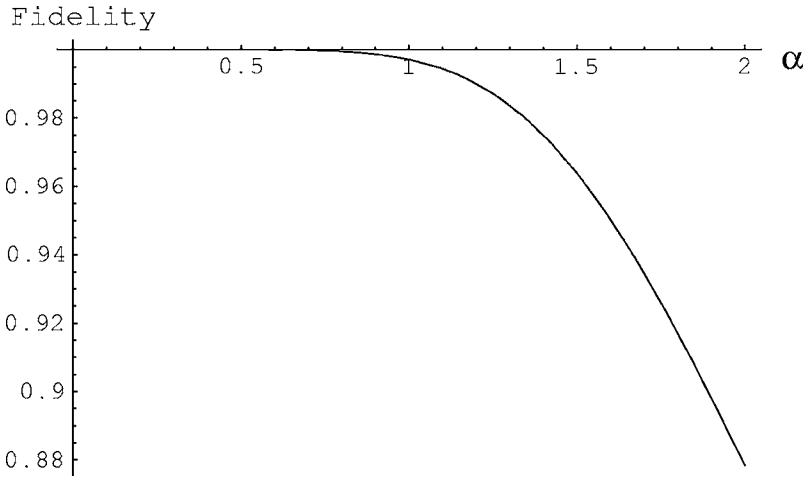

FIG. 2. The fidelity between an odd CSS and squeezed single photon. The odd CSS is extremely well approximated by the squeezed single photon for a small coherent amplitude, $\alpha \leqslant 1.2$.

$$\mathrm{d}Y\mathcal{N}_n \int_{-\infty}^{\infty} \mathrm{d}y_s e^{-(\kappa y_s)^2/2} H_n(y_s)|y_s\rangle. \tag{19}$$

This state is not normalized as the process which we have chosen to generate it is nondeterministic. For the special case of $n=1$ the normalized state is

$$\sqrt{\frac{\kappa^3}{2\sqrt{\pi}}} \int_{-\infty}^{\infty} \mathrm{d}y_s e^{-(\kappa y_s)^2/2} H_1(y_s)|y_s\rangle, \tag{20}$$

and as the Hermite polynomial $H_1(y_s)$ is linear, a κ can be moved from under the square root to inside the integral to give

$$\sqrt{\frac{\kappa}{2\sqrt{\pi}}} \int_{-\infty}^{\infty} \mathrm{d}y_s e^{-(\kappa y_s)^2/2} H_1(\kappa y_s)|y_s\rangle, \tag{21}$$

which we state is just a rescaling (or squeezing) of the momentum wave function of a single photon. So the case of a single-photon input into the QND device with the projective measurement described above is equivalent to squeezing a single-photon Fock state.

B. Squeezed single photons and ideal CSS's

We have thus been guided to comparing a single-mode squeezed-single-photon state with an odd CSS. The single-mode squeezing operator is

$$\hat{S}(r) = e^{-r(\hat{a}^2 - \hat{a}^{\dagger 2})/2}, \tag{22}$$

where r is the squeezing parameter and $\hat{a}$ is the annihilation operator. This operator reduces quantum noise of a vacuum state in the phase quadrature by a factor of e^{-r}. When the squeezing operator is applied to a single photon the resultant state can be expanded in terms of photon number states as

$$\hat{S}(r)|1\rangle = \sum_{n=0}^{\infty} \frac{(\tanh r)^n}{(\cosh r)^{3/2}} \frac{\sqrt{(2n+1)!}}{2^n n!}|2n+1\rangle. \tag{23}$$

The state contains only odd photon numbers and has coefficients decaying exponentially as n increases in a similar fashion to an odd CSS. The fidelity of this state with an odd CSS is

$$F(r,\alpha) = |\langle \mathrm{CSS\_}(\alpha)|S(r)|1\rangle|^2 = \frac{2\alpha^2 \exp[\alpha^2(\tanh r - 1)]}{(\cosh r)^3(1 - \exp[-2\alpha^2])}. \tag{24}$$

If an odd CSS of size α is desired, then the fidelity is maximized when r satisfies

$$\cosh r = \sqrt{\frac{1}{2} + \frac{1}{6}\sqrt{9 + 4\alpha^2}}. \tag{25}$$

Figure 2 shows the maximized fidelity on the y axis plotted against a range of possible values for α for the desired odd CSS. Some example values are $F=0.999\,99$ for amplitude $\alpha=1/2$, $F=0.9998$ for $\alpha=1/\sqrt{2}$, and $F=0.997$ for $\alpha=1$, where the maximizing squeezing parameters are $r=0.083$, $r=0.164$, and $r=0.313$, respectively. These values correspond to $V=0.85$, $V=0.72$, and $V=0.53$, where V is the variance of the squeezed quadrature variable. First note that for α very close to zero the fidelity approaches unity. When $\alpha \to 0$, $r \to 0$, and hence the squeezing operator $\hat{S}(r)$ approaches the identity transformation. An odd CSS with α very close to zero has a significant contribution from a single photon and very little from higher odd photon numbers. This is the reason for the high fidelity as α tends to zero. The fidelity remains high for α near zero as one can match the three-photon contribution to the CSS by the squeezing operator while still being able to neglect higher-order photon number terms. Eventually as α increases, higher photon numbers cannot be matched and so as α tends to infinity, the fidelity tends to zero.

The role of squeezing on single photons becomes clear by comparing Wigner functions of the squeezed single photons and CSS's. The Wigner function of a squeezed single photon can be obtained from its characteristic function

$$\chi_s(\eta) = \mathrm{Tr}[S(r)|1\rangle\langle 1|S^{\dagger}(r) e^{\eta \hat{a}^{\dagger} - \eta^* \hat{a}}] = \exp\left[-\frac{1}{2}(e^{2r}\eta_r^2 + e^{-2r}\eta_i^2)\right](1 - e^{2r}\eta_r^2 + e^{-2r}\eta_i^2). \tag{26}$$

The Wigner function is then

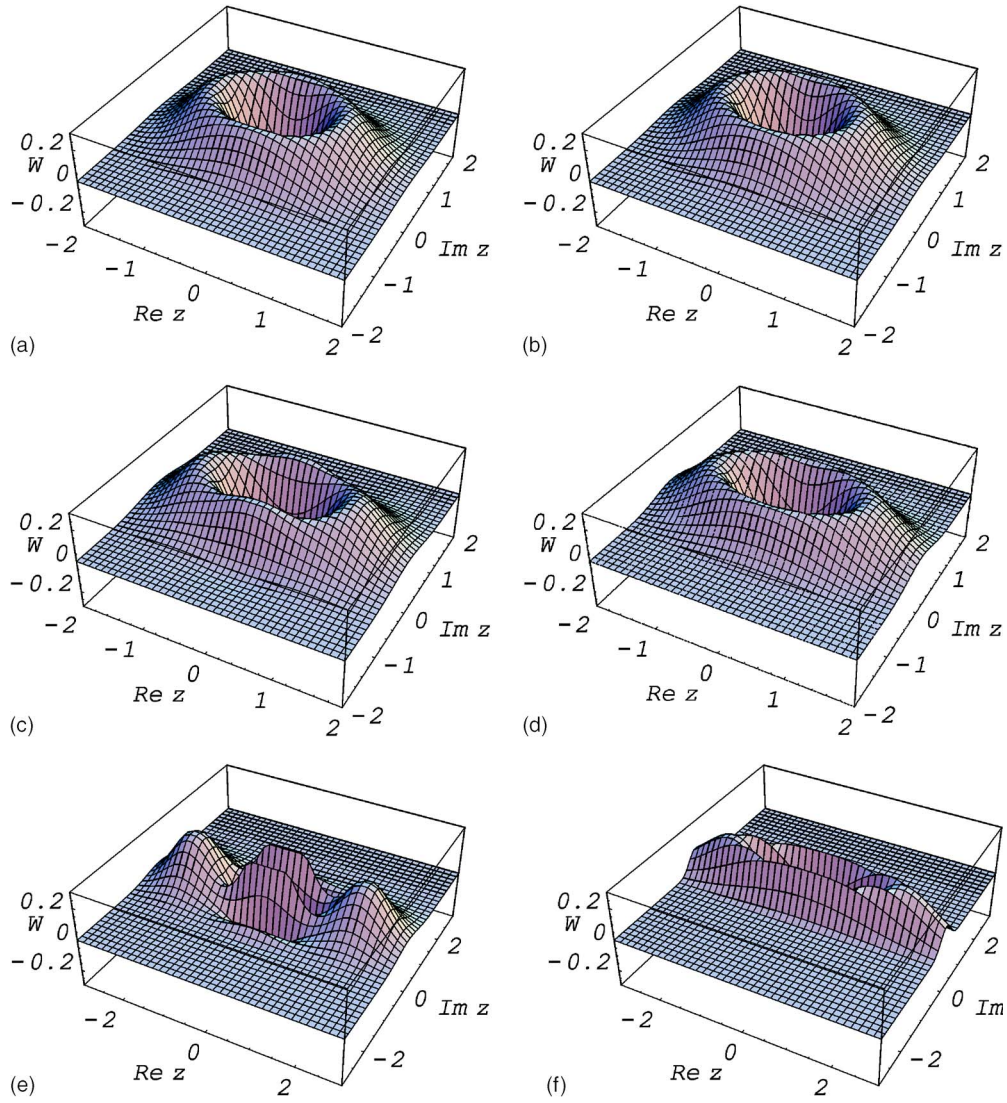

FIG. 3. (Color online) The Wigner functions of odd CSS's (left) and squeezed single photons (right). The amplitudes of CSS's are (a) $1/\sqrt{2}$, (b) 1, and (c) 2. The degrees of squeezing of squeezed single photons are (a) 0.164, (b) 0.313, and (c) 0.853, which are chosen for maximum fidelity with CSS's. It is evident from the figure that only small amount of squeezing makes a single photon a good approximate CSS.

$$W_s(z) = \frac{1}{\pi^2}\int e^{\eta^* z - \eta z^*}\chi_s(\eta)d^2\eta = \frac{2}{\pi}\exp[-2(e^{2r}z_r^2 + e^{-2r}z_i^2)] \times(4e^{2r}z_r^2 + 4e^{-2r}z_i^2 - 1). \tag{27}$$

The Wigner function of the CSS is obtained by the same method as

$$W_c^{\pm}(z) = \frac{e^{-2|z|^2}}{\pi(1 \pm e^{-2\alpha^2})}\{e^{-2\alpha^2}(e^{-4\alpha z_r} + e^{4\alpha z_r}) \pm 2\cos 4\alpha z_i\}, \tag{28}$$

where $W_c^+(z)$ $[W_c^-(z)]$ is the Wigner function of the even [odd] CSS. The Wigner functions of odd CSS's with amplitudes $1/\sqrt{2}$, 1, 2 and the Wigner functions of corresponding squeezed single photons are plotted in Fig. 3. It shows that only small amount of squeezing makes a single photon a good approximation of the odd CSS. If squeezing is too large, the CSS and squeezed single photon will become different.

IV. NONDETERMINISTIC CSS AMPLIFICATION PROCESS

In this section, we show that an arbitrarily large CSS can be produced out of arbitrarily small CSS's using the simple experimental setup depicted in Fig. 4. Let us first illustrate this procedure with a simple example. Suppose that one has a collection of identical small odd CSS's with known amplitude α_i. Two of the small CSS's are selected and are incident onto a 50:50 beam splitter, BS1, which acts on two coherent states $|\alpha\rangle$ and $|\beta\rangle$ as

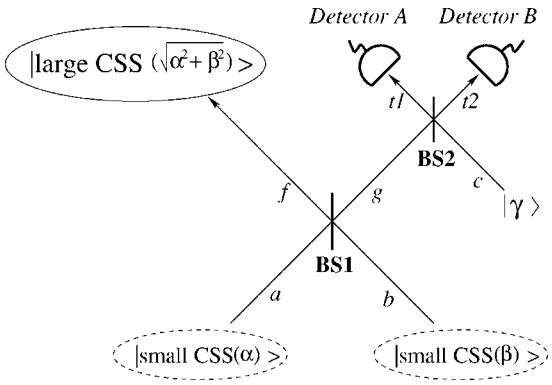

FIG. 4. A schematic of the nondeterministic CSS-amplification process. Two small CSS's at modes a and b are added to produce a larger CSS at mode f by a conditional measurement using detectors A and B. See text for details.

$$|\alpha\rangle_a|\beta\rangle_b \overset{\text{BS1}}{\rightarrow} \left|\frac{\alpha}{\sqrt{2}}+\frac{\beta}{\sqrt{2}}\right\rangle_f \left|-\frac{\alpha}{\sqrt{2}}+\frac{\beta}{\sqrt{2}}\right\rangle_g. \tag{29}$$

The two small CSS's are then transformed at BS1 as

$$\begin{aligned}|\mathrm{CSS}_-(\alpha_i)\rangle_a|\mathrm{CSS}_-(\alpha_i)\rangle_b &\overset{\text{BS1}}{\rightarrow} |0\rangle_f(|\sqrt{2}\alpha_i\rangle_g+|-\sqrt{2}\alpha_i\rangle_g)\\ &\quad -(|\sqrt{2}\alpha_i\rangle_f+|-\sqrt{2}\alpha_i\rangle_f)|0\rangle_g\\ &\propto |0\rangle_f|\mathrm{CSS}_+(\sqrt{2}\alpha)\rangle_g\\ &\quad -|\mathrm{CSS}_+(\sqrt{2}\alpha)\rangle_f|0\rangle_g,\end{aligned} \tag{30}$$

where the normalization factors are omitted on the right-hand side. One can then say that if one could condition on detecting $|0\rangle_g$, a larger CSS with amplitude $\sqrt{2}\alpha_i$ would be obtained at mode f. However, the nonzero overlap between the vacuum and the even CSS in Eq. (30) will make it impossible to perform unambiguous measurements. The error due to this overlap is not negligible because the initial amplitude α_i is supposed to be a small value. Note that if the parity of the initial CSS's are different, an unambiguous conditioning is possible using an ideal photodetector. The two small CSS's of different parity are transformed at BS1 as

$$|\mathrm{CSS}_-(\alpha_i)\rangle_a|\mathrm{CSS}_+(\alpha_i)\rangle_b$$

$$\overset{\text{BS1}}{\rightarrow} |0\rangle_f|\mathrm{CSS}_-(\sqrt{2}\alpha)\rangle_g+|\mathrm{CSS}_-(\sqrt{2}\alpha)\rangle_f|0\rangle_g. \tag{31}$$

where the normalization factor is omitted again on the right-hand side. Since the overlap between the vacuum and odd CSS is zero, a larger odd CSS, $|\mathrm{CSS}_-(\sqrt{2}\alpha)\rangle_f$, can be conditionally produced regardless of the value of α_i by detecting no photon at mode g. Even in this case, however, the resulting states of conditional measurements will be highly sensitive to detection inefficiency for small α_i. An additional step therefore is required to unambiguously discriminate between the vacuum and coherent states $|\pm\sqrt{2}\alpha_i\rangle_g$ with inefficient detectors. Another 50:50 beam splitter, BS2, mixes the field at mode g and an auxiliary coherent state $|\sqrt{2}\alpha_i\rangle_c$ as

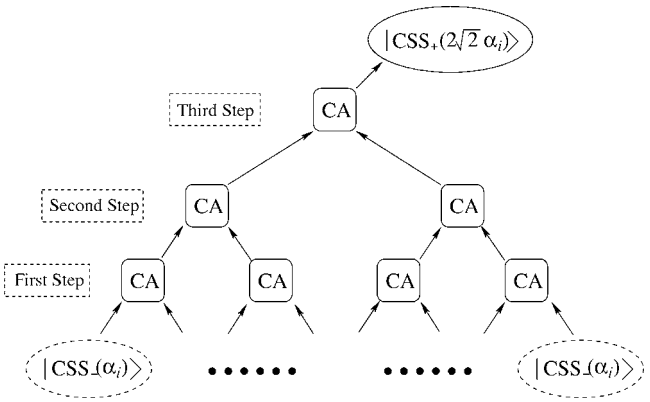

FIG. 5. A schematic of successive applications of the CSS amplification processes. CA represents the CSS amplification process depicted in Fig. 4. As the first step, eight CSS's of initianl amplitude α_i are fed into the four CA processes. If all the eight detectors in the four CA processes click, the resulting states are selected for the second step and so on. In this example, 14 detectors and 14 beam splitters are required with 7 auxiliary coherent states to distill a CSS of amplitude $2\sqrt{2}\alpha_i$ from smaller CSS's of amplitude α_i.

$$\begin{aligned}|\mathrm{BS1}\rangle_{f,g}|\sqrt{2}\alpha_i\rangle_c &\overset{\text{BS2}}{\rightarrow} |0\rangle_f(|2\alpha_i\rangle_{t1}|0\rangle_{t2}+|0\rangle_{t1}|2\alpha_i\rangle_{t2})-(|\sqrt{2}\alpha_i\rangle_f\\ &\quad +|-\sqrt{2}\alpha_i\rangle_f)|\alpha_i\rangle_{t1}|-\alpha_i\rangle_{t2},\end{aligned} \tag{32}$$

where $|\mathrm{BS1}\rangle_{f,g}$ represents the right-hand side of Eq. (30) and the normalization factor is omitted. Finally, photodetectors A and B are set to detect photons at modes $t1$ and $t2$. The remaining state at mode f is selected only when both the detectors detect any photon(s) at the same time. In this case, it is obvious that the right-hand side of Eq. (32) is reduced to a larger CSS's. If either of the detectors fails to click, the resulting state is discarded.

This process can be successively applied until a CSS of a sufficiently large amplitude is obtained. Suppose that an even CSS with amplitude $\alpha>2$ is required while the initial amplitude of small odd CSS's is $\alpha_i=1$. One may consider an experimental setup depicted in Fig. 5 to obtain a CSS of the required amplitude. Here we refer to the CSS amplification process depicted in Fig. 4 as "CA." First, four pairs of odd CSS's (i.e., eight odd CSS's) with amplitude $\alpha_i=1$ should be fed into four CA processes simultaneously as shown in Fig. 5. If the first step in Fig. 5 is successful—i.e., all the eight detectors in the first four CA processes click—two pairs of even CSS's with amplitude $\sqrt{2}\alpha_i$ will be generated out of the four pairs of smaller CSS's of amplitude α_i fed into the first four CA processes. In the second step, two CA processes are performed with the two pairs of even CSS's generated from the first step. Note that the auxiliary coherent states for the second step should be $|2\alpha_i\rangle$'s. Through this second stage, one pair of even CSS's of amplitude $2\alpha_i$ can be gained from the two pairs of even CSS's with amplitude $\sqrt{2}\alpha_i$. Finally, an even CSS with amplitude $2\sqrt{2}\alpha_i(\approx 2.83)$ can be generated by the third step which is only a single CA process with an appropriate auxiliary state. An CSS of an arbitrarily larger amplitude can be produced by increasing the number of the steps from any smaller CSS's. Of course, the success prob-

ability will rapidly drop down and the required resources will exponentially increase as the number of steps increases unless quantum optical memory is available.

The CA process described above can be generalized for arbitrarily small CSS's with known amplitudes as already shown in Fig. 4. Suppose two small CSS's, $|\mathrm{CSS}_{\varphi}(\alpha)\rangle$ and $|\mathrm{CSS}_{\phi}(\beta)\rangle$, with amplitudes α and β. The reflectivity r and transmitivity t of BS1 are set to $r=\beta/\sqrt{\alpha^2+\beta^2}$ and $t=\alpha/\sqrt{\alpha^2+\beta^2}$, where the action of the beam splitter is represented by

$$\hat{B}_{a,b}(r,t)|\alpha\rangle_a|\beta\rangle_b|t\alpha+r\beta\rangle_f|-r\alpha+t\beta\rangle_g. \tag{33}$$

The other beam splitter BS2 is a 50:50 beam splitter ($r=t=1/\sqrt{2}$) regardless of the conditions and the amplitude γ of the auxiliary coherent field is determined as

$$\gamma=2\alpha\beta/\sqrt{\alpha^2+\beta^2}. \tag{34}$$

The two beam splitters BS1 and BS2 then transform the two small CSS's with the auxiliary state as

$$\begin{aligned}\hat{B}_{g,c}\left(\frac{1}{\sqrt{2}},\frac{1}{\sqrt{2}}\right)\hat{B}_{a,b}\left(\frac{\beta}{\sqrt{\alpha^2+\beta^2}},\frac{\alpha}{\sqrt{\alpha^2+\beta^2}}\right)&\\ \times|\mathrm{CSS}_{\varphi}(\alpha)\rangle_a|\mathrm{CSS}_{\phi}(\beta)\rangle_b|\gamma\rangle_c=\Bigg\{(|\mathcal{A}\rangle+e^{i(\varphi+\phi)}|-\mathcal{A}\rangle)&\\ \times\left|\frac{\gamma}{\sqrt{2}}\right\rangle\left|\frac{\gamma}{\sqrt{2}}\right\rangle+e^{i\phi}\left|\frac{\alpha^2-\beta^2}{\mathcal{A}}\right\rangle|0\rangle|\sqrt{2}\gamma\rangle&\\ +e^{i\varphi}\left|-\frac{\alpha^2-\beta^2}{\mathcal{A}}\right\rangle|\sqrt{2}\gamma\rangle|0\rangle\Bigg\}_{f,t1,t2}\equiv|\Phi\rangle,&\end{aligned} \tag{35}$$

where $\mathcal{A}=\sqrt{\alpha^2+\beta^2}$. Here, the measurement operator $\hat{P}_{t1,t2}$ can be represented as

$$\hat{P}_{t1,t2}=(\mathbb{1}-|0\rangle\langle 0|)_{t1}\otimes(\mathbb{1}-|0\rangle\langle 0|)_{t2}. \tag{36}$$

It is then obvious from Eq. (35) that the resulting state for mode f by the "click-click" event at $t1$ and $t2$ becomes $|\mathrm{CSS}_{\varphi+\phi}(\mathcal{A})\rangle\propto|\mathcal{A}\rangle+e^{i(\varphi+\phi)}|-\mathcal{A}\rangle$, whose coherent amplitude $\mathcal{A}=\sqrt{\alpha^2+\beta^2}$ is larger than both α and β. The relative phase of the resulting CSS is the sum of the relative phases of the input CSS's. The success probability $P_{\varphi,\phi}(\alpha,\beta)$ for a single iteration of the process above is simply calculated as

$$\begin{aligned}P_{\varphi,\phi}(\alpha,\beta)&=\langle\Phi|\hat{P}_{t1,t2}|\Phi\rangle\\ &=\frac{(1-e^{-2\alpha^2\beta^2/(\alpha^2+\beta^2)})^2[1+\cos(\varphi+\phi)e^{-2(\alpha^2+\beta^2)}]}{2(1+\cos\varphi e^{-2\alpha^2})(1+\cos\phi e^{-2\beta^2})},\end{aligned}$$

which is plotted for a number of different combinations in Fig. 6. The success probabilities depend on the type of CSS's (odd or even) used and they approach 1/2 as the amplitudes of the initial CSS's becomes large. It is interesting to note that the probability $P_{\pi,\pi}(\alpha,\alpha)$ for two identical odd CSS inputs is always larger than ~ 0.214 regardless of the value of α as shown in Fig. 6. This is due to the fact that each odd CSS contains at least one photon no matter how small its amplitude is. Multiple iterations will rapidly reduce the success probability. For example, if one needs to distill a CSS of $\alpha=2$ out of 4 CSS's of $\alpha=1$ ($\alpha=1/\sqrt{2}$), the success probability will be ~ 0.027 (4×10^{-4}). If a CSS of $\alpha=2$ is desired out of 16 odd CSS's of $\alpha=1/2$, the success probability will be only 2×10^{-13}. However, if quantum memory is available, one can temporarily hold the output state upon success waiting for the remainder of the trials to give a successful result. This avoids the exponential scaling of the overall probability of success and for the $\alpha=2$ case just considered the average number of steps is 1731. The inefficiency of photodetectors will also decrease the success probability while it does not affect the quality of the obtained CSS's.

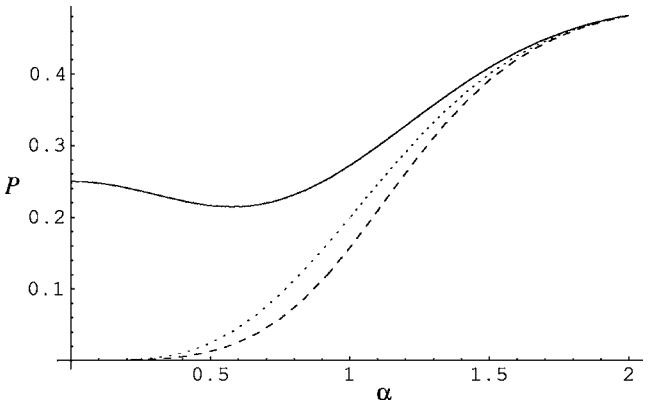

FIG. 6. The success probabilities of the CSS-amplifying process in Fig. 4 for the input fields of two identical odd CSS's (solid line), two identical even CSS's (dashed line), and even and odd CSS's (dotted line).

It is worth noting that not only an arbitrary large even CSS but also an arbitrarily large odd CSS can be obtained out of small odd CSS's. If a larger odd CSS needs to be produced, a larger even CSS obtained from a collection of initial odd CSS's and a single initial odd CSS can be fed into a CA process so that a larger odd CSS can be obtained. If the even CSS of amplitude $2\sqrt{2}$ obtained and the initial odd cat of amplitude 1 are used as the two input states in Fig. 4, an odd CSS of amplitude 3 will then be obtained.

We have pointed out that a small CSS approaches a single photon while a larger CSS is a superposition of macroscopically distinguishable states which can be considered a realization of Schrödinger's paradox. This means that, in principle, our scheme distills a superposition of macroscopically distinguishable states from microscopic quantum states. It also increases nonclassical features of quantum states. The negativity of Wigner functions is an indicator of the nonclassical features of a quantum state. Since an even CSS approaches the vacuum state as its amplitude gets smaller and the Wigner function of the vacuum state is positive definite, the maximum negative value of the Wigner function is small for a small even CSS. In this regime of a small amplitude, the Wigner function of an even CSS looks almost like a Gaussian state. Figure 7 shows how the maximum negative value of the Wigner function of an even CSS increases as our amplification process is iterated.

V. AMPLIFYING SQUEEZED SINGLE PHOTONS FOR LARGER COHERENT-STATE SUPERPOSITIONS

In our earlier discussions, it was shown that the fidelity between a squeezed single photon and an ideal small cat is

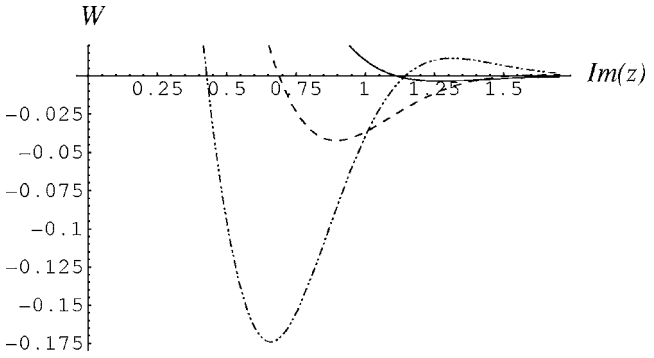

FIG. 7. section of the Wigner function for an initial even CSS of amplitude 1/2 (solid line), the resulting CSS after the first iteration (dashed line), and the resulting state after the second iteration (dotted line). The maximum negative values are shown in the figure. One can see a radical increase of negativity of the Wigner function.

extremely high. Therefore, it can be conjectured that a larger CSS distilled from squeezed single photons by our scheme will also be very close to an ideal CSS. In what follows, we will show that this conjecture is right for $\alpha \leqslant 2.5$ by analytical and numerical approximations. We first choose the initial coherent amplitude as $\alpha_i = 1/\sqrt{2}$. The fidelity of the initial CSS, which is the squeezed single photon, is then $F = 0.999\,78$ for the appropriate squeezing parameter $r = 0.163\,725$.

The squeezed single photon can be represented in terms of an ideal CSS and error components as $S(r)|1\rangle \propto |\mathrm{CSS}\_(1/\sqrt{2})\rangle + \delta^{(3)}|3\rangle + \delta^{(5)}|5\rangle + \delta^{(7)}|7\rangle + \cdots$, where the error terms are

$$\delta^{(2k+1)} = \frac{e^{1/4}[0.162278^k(2k+1)\,! - k\,!\,]}{2^k k\,!\,\sqrt{(2k+1)\,!\,(e-1)}}. \tag{37}$$

It can be simply checked that $\delta^{(5)} = 0.012\,966\,9$ is the dominant error term and $\delta^{(k)}$ exponentially decreases for $k > 5$. The state only with $\delta^{(5)}$, $N(|\mathrm{CSS}\_(1/\sqrt{2})\rangle + \delta^{(5)}|5\rangle)$, where N is the normalization factor, will give a fidelity $F = 0.999\,83$ for the odd CSS $|\mathrm{CSS}\_(1/\sqrt{2})\rangle$. In other words, the state only with the dominant error term can be a good approximation of the squeezed single photon for a weak squeezing. We therefore use

$$S(r)|1\rangle \approx |\Psi_i\rangle = N_i(|\mathrm{CSS}\_(1/\sqrt{2})\rangle + \delta_i|5\rangle) \tag{38}$$

as the initial input state, where $r = 0.163\,725$, $\delta_i = 0.0147$, and N_i is a normalization factor. The initial fidelity F_i between $|\Psi_i\rangle$ and the ideal odd CSS is made, $F_i = 0.999\,78$, which is exactly same as the case of a squeezed single photon. The resulting state is obtained as

$$|\Psi_{(1)}\rangle_{f,t1,t2} = \hat{P}_{t1,t2}\hat{B}^{1:1}_{g,c}\hat{B}^{1:1}_{a,b}|\Psi_i\rangle_a|\Psi_i\rangle_b|\sqrt{2}\alpha_i\rangle_c, \tag{39}$$

$$\rho_{(1)f} = \mathrm{Tr}_{t1,t2}[|\Psi_{(1)}\rangle\langle\Psi_{(1)}|], \tag{40}$$

where $\mathrm{Tr}_{t1,t2}$ denotes a partial trace of modes $t1$ and $t2$, a subscript (n) indicates the number of the iterative steps made to amplify the CSS, and $\hat{B}^{1:1} = \hat{B}(1/\sqrt{2}, 1/\sqrt{2})$.

When each of the detectors detects only one photon, it is straightforward to calculate the resulting state

$${}_{t1}\langle 1|_{t2}\langle 1|\Psi_{(1)}\rangle \propto |\mathrm{CSS}_+(1)\rangle - 1.11\,\delta_i(0.828|4\rangle - 0.561|6\rangle), \tag{41}$$

where error terms smaller than 1/3 of the dominant error term have been discarded as they exponentially decay. Considering the normalization, the fidelity of the state (41) is calculated to be 0.999 74. Note that about 60% of all the successful simultaneous clicks at detectors A and B correspond to this case, where the probability can be calculated by $P^{n,m}_{(n)} = \langle n|\langle m|\rho_{(n)f}|n\rangle|m\rangle$. About 30% of the successful clicks correspond to the cases that detector A detects two photons while detector B detects one photon or that A detects one while B detects two photons. We can make a same approximation for these cases and the fidelity is 0.999 75. On the other hand, the highest overlap with a CSS of $\alpha = 1$ that can be obtained by simply squeezing a single photon is $F = 0.997\,11$; thus, a clear improvement has been obtained.

In order to calculate multiple iterations we need to use numerical techniques. We are using coherent states of some bounded coherent amplitude and superpositions there of. Provided the coherent amplitudes are not small, the most significant contributions to these states are Fock states of low number. For computations here the lowest 30 Fock states were used. This provides a very good approximation for coherent states with $\alpha \leqslant 2.5$. All 29 possible "click" events are included for all detectors.

If one wished to create a CSS with a particular α with n CSS-amplification steps, then initial CSS's with $\alpha_i = \alpha/\sqrt{2^n}$ are required. As the number of steps increases the required α_i decreases. When generating a larger CSS out of the squeezed-single-photon states the fidelity maximizes for a particular number of iterations. Figure 8 shows the maximum possible fidelity using this process in (a) and the number of steps in (b) against the desired α in the CSS's. For example, four iterations starting from the initial amplitude $\alpha_i = 1/2$ are required to gain the maximum fidelity $F = 0.995$ for $\alpha = 2$. It is evident from Fig. 4 that high fidelity, $F > 0.99$, can be obtained up to $\alpha = 2.5$. The error rate for discrimination between coherent states with $\alpha = \pm 2.5$ via a classical measurement (homodyne detection) is only 3×10^{-7}.

VI. PURIFICATION EFFECTS OF THE CSS-AMPLIFICATION PROCESS

The single photons required for our scheme could be generated conditionally from a downconverter [36]. This is a $\chi^{(2)}$ process (like squeezing) and does not require photon number resolving detection. It should be noted that current technology does not produce pure single-photon states; the single photon is always in a mixture with the vacuum as

$$p|0\rangle\langle 0| + (1-p)|1\rangle\langle 1|, \tag{42}$$

where p is the inefficiency of the photon production. Hence the squeezed-single-photon state will also be a mixture with a squeezed vacuum as

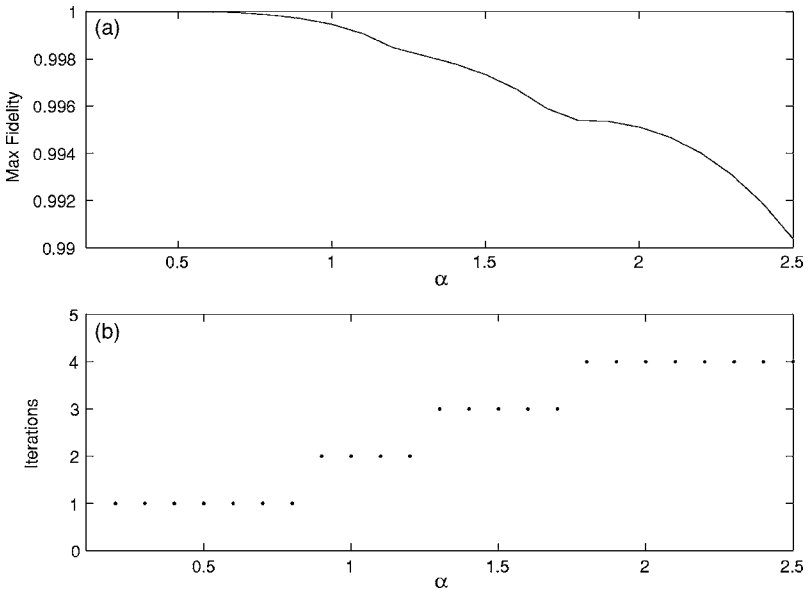

FIG. 8. (a) The maximum fidelity obtained in our scheme vs the coherent amplitude. (b) The number of iterations which gives the maximum fidelity vs the coherent amplitude. The improvements of the fidelity are remarkable when compared with Fig. 2.

$$p\hat{S}(r)|0\rangle\langle 0|\hat{S}^{\dagger}(r) + (1-p)\hat{S}(r)|1\rangle\langle 1|S^{\dagger}(r). \tag{43}$$

However, an interesting aspect of our scheme is that it may be somewhat resilient to the photon production inefficiency because its first iteration purifies the mixed CSS's while amplifying them. The initial input states for the CSS-amplification process from the imperfect single-photon source are

$$\rho_{a,b,c} = [(1-p)^2|S_1\rangle\langle S_1| \otimes |S_1\rangle\langle S_1| + p^2|S_0\rangle\langle S_0| \otimes |S_0\rangle\langle S_0| + p(1-p)(|S_0\rangle\langle S_0| \otimes |S_1\rangle\langle S_1| + |S_1\rangle\langle S_1| \otimes |S_0\rangle\langle S_0|)]_{a,b} \otimes (|\gamma\rangle\langle\gamma|)_c, \tag{44}$$

where $|S_0\rangle = \hat{S}(r)|0\rangle$ and $|S_1\rangle = \hat{S}(r)|1\rangle$. Here, the terms with p^2 and $p(1-p)$ are undesired error terms where either (or both) of the single photons is missing. Note that the initial amplitude is required to be small to produce a larger CSS with high fidelity. Provided such a small amplitude, input states incident onto the beam splitters in our experimental setup contain approximately only two (or slightly more than two) photons. In such cases the probability of simultaneous clicks at detectors A and B in Fig. 4 will significantly decrease when any of the single photons is missing. In other words, the undesired cases will rarely be selected for the next iteration of the amplification process. We have obtained numerical results for the initial amplitude $\alpha_i = 1/2$ as follows by the methods that we have already explained. If $p=0.4$, the fidelity of the initial CSS, which is a mixture with a squeezed vacuum, is $F=0.60$ but it will become $F=0.89$ by the first iteration. Thus a larger CSS of significantly high fidelity is produced. If $p=0.25$ ($p=0.05$), the fidelity of the initial CSS is $F=0.750$ ($F=0.950$) but becomes $F=0.941$ ($F=0.990$) by the first iteration.

The purification by the first iteration is directly evident by the probability argument, but what remains to be shown is if this effect is strong enough for purification to still be achieved for multiple iterations. For a double iteration, four input CSS's of $\alpha_i = 1/2$ would be required to obtain an output CSS of $\alpha = 1$. The numerical results of the second iteration presented in Fig. 9 show that the improvements of fidelity obtained by the first step can remain for further iterations. In Fig. 9(a), the purity of the input state (solid line) and the purity of the output state after the first (dot-dashed line) and second (dashed line) iterations have been plotted as functions of the photon production inefficiency p. Note that purity is defined here as $\mathrm{Tr}\{\hat{\rho}^2\}$. Figure 9(b) shows the fidelity of the input state when compared with the ideal CSS of $\alpha = 1/2$ (solid line), the fidelity of the output state after the first iteration compared with the CSS of $\alpha = 1/\sqrt{2}$ (dot-dashed line), and the fidelity of the output state (dashed line) compared with the ideal CSS of $\alpha = 1$. When $p=0$ the purity and fidelity are high as the input states themselves are pure and the output fidelity is expected to be high. The fidelity has decreased compared with the result after the first iteration but it is still higher than the initial fidelity. For example, the fidelity will change from 0.60 to 0.89 for the first iteration and finally to 0.72 for the second iteration when $p=0.4$. For the range of probabilities shown here ($p \in [0, 0.5]$) there is always an improvement in purity and fidelity.

There exists an alternate way of achieving the same output state using the same input CSS's but using a different arrangement of amplification procedures. Two $\alpha = 1/2$ odd input CSS's could be amplified to generate one even $\alpha = \sqrt{1/2}$ CSS. Then this state could be combined with another $\alpha = 1/2$ odd CSS to create a $\alpha = \sqrt{3/4}$ odd CSS. Then finally this state could be combined with another $\alpha = 1/2$ odd CSS to generate the $\alpha = 1$ even CSS output. One might expect that the presence of the $\alpha = \sqrt{3/4}$ odd CSS could make some differences in purity and fidelity by this method. However, the plots for the final output state which we have obtained by the same numerical technique are identical in nature to those of Fig. 9. So the purifying effects of this procedure do not seem to depend on the way in which the output state is generated.

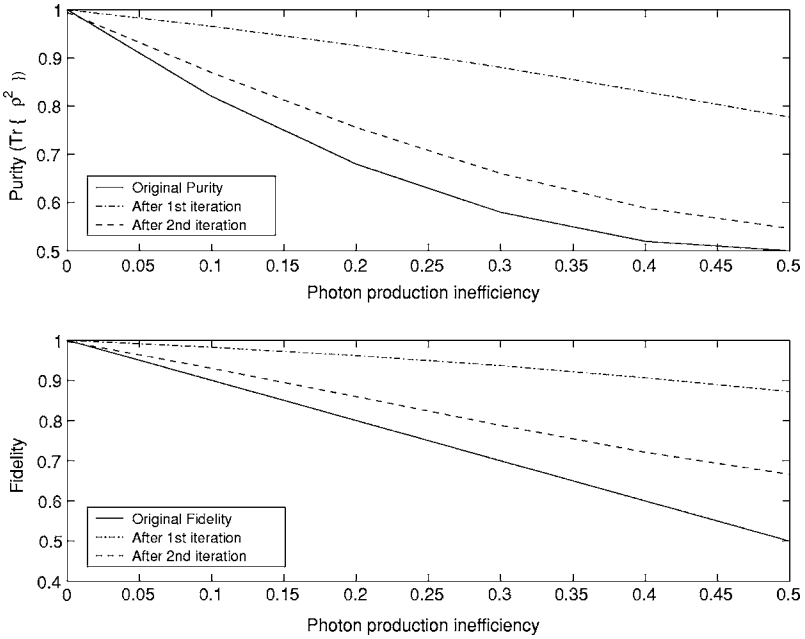

FIG. 9. (a) Purity and (b) fidelity of the input state (solid lines), the input output state after the first iteration (dot-dashed lines), and of the output after the second iteration (dashed line) as functions of the photon production inefficiency p. The input states are mixed squeezed single photons intended to be approximate odd CSS's of amplitude $\alpha=1/2$. The final output states should be therefore approximate CSS's of $\alpha=1$.

VII. REMARKS

We have studied a simple all-optical scheme to generate a linear superposition of macroscopically distinguishable coherent states in a propagating optical field [24]. In stark contrast to all previous schemes, this scheme requires neither $\chi^{(3)}$ nonlinearity nor efficient photon detection to generate a superposition of macroscopically distinguishable states. Furthermore, it exhibits some resilience to photon production inefficiency because it purifies initial mixed states. We have found that these purification effects can last for multiple iterations. The nondeterministic CSS amplification scheme has been proved to boost the nonclassicality of quantum states: even a very small amount of negativity can be drastically increased by this process. This scheme nondeterministically generates CSS's with amplitude $\alpha>2$. However, it should be noted that a nondeterministic CSS source is useful enough for quantum information processing [10,11].

In the CSS-amplification process, the zero-amplitude coherent states that occur in the detection modes in Eq. (32) may be slightly different from zero because of imperfect mode matching at beam splitters. This will lead to a small probability of accepting the wrong state. Good mode matching is a requirement in any linear optical network where one wishes to measure manifestly quantum-mechanical effects. Highly efficient mode matching of a single photon from parametric down-conversion and a weak coherent state from an attenuated laser beam at a beam splitter has been experimentally demonstrated using optical fibers [38]. Such techniques could be employed for the implementation of our scheme.

The dark count rate of photodetectors will affect the fidelity of the CSS's. Currently, highly efficient detectors have relatively high dark count rates while less efficient detectors have very low dark count rates [37]. We emphasize again that our scheme does not require highly efficient detectors because the inefficiency of the detectors does not affect the quality of CSS's even though it decreases the success probability. Silicon avalanche photodiodes operating at the visible wavelength have relatively high efficiency and a small dark count rate, which is preferred in our proposal.

Once free propagaing CSS states are generated, they can be detected by homodyne measurements, which can be highly efficient in quantum optics experiments. Interference fringes will appear as a signature of the CSS's in the statistics of the photocurrent at the detectors.

Finally, we note that there is an alternative method to obtain a squeezed-single-photon even without a single-photon source. It is perhaps not surprising that a squeezed single photon can be obtained by adding a photon to a squeezed vacuum as $\hat{a}^{\dagger}S(r)|0\rangle=\sinh rS(r)|1\rangle$. However, an interesting observation is that a squeezed single photon can also be obtained by subtracting a photon from a squeezed vacuum. This can be shown by applying the annihilation operator to a squeezed single photon:

$$\hat{a}S(r)|0\rangle=\cosh rS(r)|1\rangle. \tag{45}$$

It was already pointed out that a photon-subtracted or photon-added squeezed vacuum state is similar to a CSS [25]. Recently, a free-propagating non-Gaussian optical state which is close to a squeezed single photon in Eq. (45) was experimentally deomonstrated by Wenger *et al.* [26]. In their experiment, the single-photon subtraction was approximated by a beam splitter of low reflectivity and a single-photon detector. Such an experiment could be immediately linked to our suggestion to experimentally generate a larger CSS. One can then generate a CSS of $\alpha>2$ using our scheme without a single-photon source.

ACKNOWLEDGMENTS

We would like to thank M.S. Kim for useful comments. This work was supported by the Australian Research Council and the University of Queensland Excellence Foundation.

[1] E. Schrödinger, Naturwiss. **23**, 807 (1935); **23**, 823 (1935); **23**, 844 (1935).
[2] A. J. Leggett and A. Garg, Phys. Rev. Lett. **54**, 857 (1985).
[3] M. D. Reid, Quantum Semiclassic. Opt. **9**, 489 (1997); Phys. Rev. Lett. **84**, 2765 (2000); Phys. Rev. A **62**, 022110 (2000); e-print quant-ph/0101052.
[4] S. J. van Enk and O. Hirota, Phys. Rev. A **64**, 022313 (2001).
[5] H. Jeong, M. S. Kim, and J. Lee, Phys. Rev. A **64**, 052308 (2001).
[6] X. Wang, Phys. Rev. A **64**, 022302 (2001).
[7] Nguyen Ba An, Phys. Rev. A **68**, 022321 (2003).
[8] Nguyen Ba An, Phys. Rev. A **69**, 022315 (2004).
[9] H. Jeong and M. S. Kim, Phys. Rev. A **65**, 042305 (2002).
[10] T. C. Ralph, W. J. Munro, and G. J. Milburn, Proc. SPIE **4917**, 1 (2002); e-print quant-ph/0110115.
[11] T. C. Ralph, A. Gilchrist, G. J. Milburn, W. J. Munro, and S. Glancy, Phys. Rev. A **68**, 042319 (2003).
[12] H. Jeong and M. S. Kim, Quantum Inf. Comput. **2**, 208 (2002);J. Clausen, L. Knöll, and D.-G. Welsch, Phys. Rev. A **66**, 062303 (2002).
[13] P. T. Cochrane, G. J. Milburn, and W. J. Munro, Phys. Rev. A **59**, 2631 (1999);S. Glancy, H. M. Vasconcelos, and T. C. Ralph, *ibid.* **70**, 022317 (2004).
[14] B. Yurke and D. Stoler, Phys. Rev. Lett. **57**, 13 (1986).
[15] R. W. Boyd, J. Mod. Opt. **46**, 367 (1999).
[16] S. Song, C. M. Caves, and B. Yurke, Phys. Rev. A **41**, R5261 (1990).
[17] M. Dakna, T. Anhut, T. Opatrný, L. Knöll, and D.-G. Welsch, Phys. Rev. A **55**, 3184 (1997).
[18] M. Dakna, J. Clausen, L. Knöll and D.-G. Welsch, Phys. Rev. A **59**, 1658 (1999);J. Clausen, M. Dakna, L. Knöll and D.-G. Welsch, Opt. Commun. **179**, 189 (2000).
[19] J. Clausen, M. Dakna, L. Knöll, and D.-G. Welsh, Acta Phys. Slov. **49**, 96 (1999).
[20] A. Montina and F. T. Arecchi, Phys. Rev. A **58**, 3472 (1998).
[21] Q. A. Turchette, C. J. Hood, W. Lange, H. Mabuchi, and H. J. Kimble, Phys. Rev. Lett. **75**, 4710 (1995).
[22] M. Brune, E. Hagley, J. Dreyer, X. Maître, A. Maali, C. Wunderlich, J. M. Raimond, and S. Haroche, Phys. Rev. Lett. **77**, 4887 (1996).
[23] C. Monroe, D. M. Meekhof, B. E. King, and D. J. Wineland, Science **272**, 1131 (1996).
[24] A. P. Lund, H. Jeong, T. C. Ralph, and M. S. Kim, Phys. Rev. A **70**, 020101(R) (2004).
[25] D.-G. Welsch, M. Dakna, L. Knöll, and T. Opatrny, e-print quant-ph/9708018.
[26] J. Wenger, R. Tualle-Brouri, and P. Grangier, Phys. Rev. Lett. **92**, 153601 (2004).
[27] E. Schrödinger, Naturwiss. **14**, 664 (1926).
[28] S. M. Barnett and P. M. Radmore, *Methods in Theoretical Quantum Optics* (Oxford University Press, New York, 1997).
[29] S. M. Barnett, C. R. Gilson, and M. Sasaki, e-print quant-ph/0209138.
[30] S. Iblisdir, G. Van Assche, and N. J. Cerf, e-print quant-ph/0312018.
[31] L. M. Johansen, e-print quant-ph/0309025.
[32] F. De Martini, Phys. Rev. Lett. **81**, 2842 (1998);F. De Martini, M. Fortunato, P. Tombesi, and D. Vitali, Phys. Rev. A **60**, 1636 (1999).
[33] A. La Porta, R. E. Slusher, and B. Yurke, Phys. Rev. Lett. **62**, 28 (1989).
[34] A. P. Lund, Honours thesis, Department of Physics, University of Queensland, Brisbane, 2004.
[35] A. M. Brańczyk, T. J. Osborne, A. Gilchrist, and T. C. Ralph, Phys. Rev. A **68**, 043821 (2003).
[36] A. I. Lvovsky, H. Hansen, T. Aichele, O. Benson, J. Mlynek, and S. Schiller, Phys. Rev. Lett. **87**, 050402 (2001).
[37] S. Takeuchi, J. Kim, Y. Yamamoto, and H. H. Hogue, Appl. Phys. Lett. **74**, 1063 (1999).
[38] T. B. Pittman and J. D. Franson, Phys. Rev. Lett. **90**, 240401 (2003).